Mechanistic insights from mass spectrometry: examination of the elementary steps of catalytic reactions in the gas phase

Krista L. Vikse and J. Scott McIndoe

2015

This article was originally published at:

http://dx.doi.org/10.1515/pac-2014-1118

Conference paper

Krista L. Vikse* and J. Scott McIndoe*

Mechanistic insights from mass spectrometry: examination of the elementary steps of catalytic reactions in the gas phase

Abstract: Real-time mass spectrometric monitoring of speciation in a catalytic reaction while it is occurring provides powerful insights into mechanistic aspects of the reaction, but cannot be expected to elucidate all details. However, mass spectrometers are not limited just to analysis: they can serve as reaction vessels in their own right, and given their powers of separation and activation in the gas phase, they are also capable of generating and isolating reactive intermediates. We can use these capabilities to help fill in our overall understanding of the catalytic cycle by examining the elementary steps that make it up. This article provides examples of how these simple reactions have been examined in the gas phase.

Keywords: catalysis; gas-phase; ICPOC-22; mass spectrometry; mechanism; organometallic.

DOI 10.1515/pac-2014-1118

Introduction

This account seeks to highlight the utility of electrospray ionization mass spectrometry as not just a means of analyzing catalytic reactions, but as a vessel for performing them. Examining the contents of a catalytic reaction, and better yet, measuring the dynamics of that reaction, can provide powerful insights into reactivity. However, even in a best-case scenario, detection of all relevant species is unlikely due to the vanishingly low abundance of some intermediates. In such cases, the ESI mass spectrometer has more tricks up its sleeve: some of these compounds can be generated and isolated in the gas-phase, and further interrogated through assessing their gas-phase reactivity. In this way the catalytic cycle can be fleshed out more fully and is set up nicely to mesh with the natural complementarity of computational methods.

We will be far from comprehensive in our coverage, instead highlighting some illustrative examples of the types of study that have been performed to date. Organizationally, the paper begins with a quick look at real-time monitoring of catalytic reactions, before describing various types of elementary reactions important in catalysis that have been studied in the gas phase using mass spectrometric techniques.

Article note: A collection of invited papers based on presentations at the 22nd IUPAC International Conference on Physical Organic Chemistry (ICPOC-22), Ottawa, Canada, August 10–15, 2014.

***Corresponding authors: Krista L. Vikse,** Laboratorium für Organische Chemie, ETH Zürich, HCI G 220, Vladimir-Prelog-Weg 2, 8093 Zürich, Switzerland, e-mail: krista.vikse@org.chem.ethz.ch; and **J. Scott McIndoe:** Department of Chemistry, University of Victoria, P.O. Box 3065 Victoria, BC V8W3V6, Canada, Tel: +1 (250) 721-7181, Fax: +1 (250) 721-7147, E-mail: mcindoe@uvic.ca

Real-time monitoring of catalytic reactions

There are some unique challenges associated with studying catalytic reactions by ESI-MS. Catalysts by their very nature are highly reactive, and coupled with the low concentrations typically employed in ESI-MS analysis, they are highly susceptible to decomposition through unwanted reactions with low concentrations of unwanted impurities, including oxygen and moisture from the atmosphere. In terms of how to conduct these experiments successfully, we have covered the practical aspects – especially as practiced in our own laboratory – in a recent review [1]. The review covers issues such as cross-contamination, avoiding aggregation [2], protection from oxygen and water [3], ensuring the softest possible ionization [4], analysis in non-polar solvents such as toluene and hexane [5], selection of counter-ions and the design of charged tags [6, 7], and the pressurized sample introduction method for continuous reaction monitoring [8]. Readers interested in these issues should sample the appropriate papers or go straight to the review for an overview of the problems and solutions.

While ESI-MS has been widely used to sample catalytic reactions [9–11], its use in real-time continuous monitoring has been a rather more recent phenomenon. There are numerous ways of delivering solution continuously to the mass spectrometer, though doing so while preserving any reactive species is best done without exposure to a standard pump (high internal volume, exposure to a variety of complicating materials, etc.). Plattner has showed that a reactor can be sampled using a fishing tube and appropriate plumbing to handle the high pressures employed; sampling could be performed at regular intervals, as fast as 1 spectrum/min, depending on the rate of the reaction in question [12]. Kozwinowski showed it was possible to set up catalytic reactions in a syringe, and infuse directly into an ESI-MS in order to probe the overall rates as informed by the relative abundance of charged tags (Fig. 1) [13].

We introduced pressurized sample infusion (PSI) [8, 14] as a means of enabling real-time analysis of catalytic reactions, and have applied it to a variety of different systems. It has the beneficial properties of being able to be applied to entirely ordinary reaction flasks at any temperature up to reflux, and exhibits excellent point-to-point reproducibility. The data shown in Fig. 2 is for the hydrodehalogenation of an aryl iodide, and in addition to measuring the relative abundance of starting material and product, the abundance of two key palladium-containing intermediates is also tracked throughout [15].

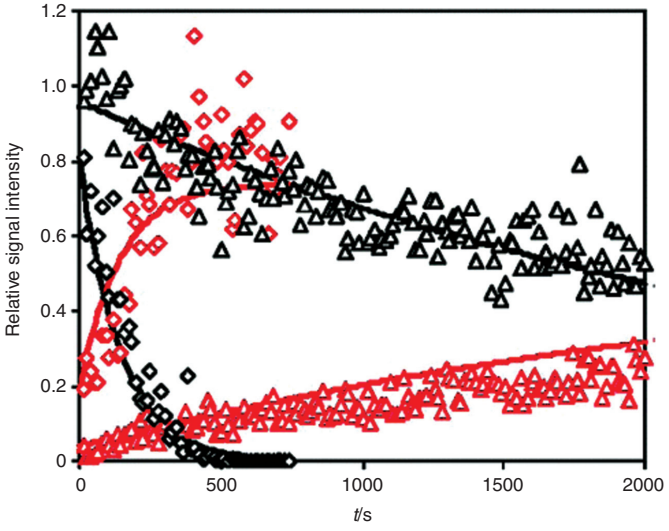

Fig. 1: Time dependence of the normalized signal intensities of reactant $[ArI]^+$ (*m/z* 262, black) and product $[ArBn]^+$ (*m/z* 226, red) formed in the Pd-catalyzed cross-coupling reaction with BnZnBr in CH_3CN at room temperature as determined by ESI mass spectrometry. Results of two experiments with different catalyst loadings are shown (◊ = 100 mol%, Δ = 5 mol% relative to $[ArI]^+$). Reprinted with permission from reference [13]. Copyright 2010 American Chemical Society.

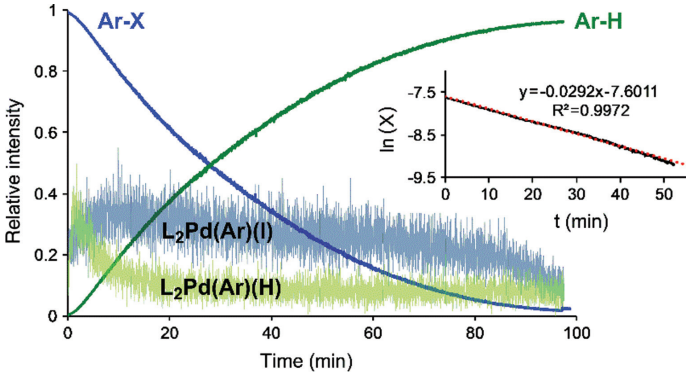

Fig. 2: Each line plots the relative intensity of the indicated component (average of three runs). Intermediates have been multiplied by 100 to get them on the same scale. Inset: plot of ln[X] vs. t, showing the overall first-order kinetics. Reprinted with permission from reference [15] – published by the Royal Society of Chemistry.

Gas-phase reactions

Performing gas-phase reactivity experiments within a mass spectrometer is quite a foreign idea to most organometallic chemists, but there are a number of convincing reasons why they should be considered as a potential source of valuable information. Highly reactive catalytic intermediates or species that always exist in equilibrium in solution can be generated or transferred into the gas-phase where they are often stable for long enough to be isolated as a pure sample. Once isolated, the inherent reactivity of that single species can be unambiguously determined. Furthermore, since the reactions are conducted in the absence of solvent or counter ions these experiments can often help clarify the effects of these complicating factors. The simplest gas-phase reactions can be performed on commercial mass spectrometers and these alone can furnish valuable insights into a catalytic process, but it is also possible to go much further. By modifying a mass spectrometer to allow the controlled introduction of gaseous reagents and by accurately measuring ion energy and pressure within the various compartments of the mass spectrometer quantitative thermochemical data for elusive elementary reaction steps can be experimentally determined. The activation energies obtained in this fashion are directly comparable to theoretical calculations since they occur in a vacuum. So, in addition to gaining energetic information about a single process the results can also be used to benchmark computational methods with reactive organometallic systems that are directly relevant to catalysis. The appropriate verification of computational methods is becoming increasingly important as chemists begin to rely heavily on these theoretical models to describe and predict reactivity.

Gas phase reactivity studies by mass spectrometry are many and diverse, so here we will be focusing on just a few: the elementary steps that typically make up a catalytic organometallic reaction. Our coverage will be far from comprehensive; in particular, we will be focusing on examples that will be most recognizable to the solution-phase chemist. We will highlight examples primarily from our own laboratories – and will focus on metal complexes that are ligated and have a “normal” oxidation state (i.e. one that is accessible in solution). Those interested in more exotic examples (e.g., naked or highly coordinatively unsaturated metal ions) are directed to excellent reviews on this fascinating topic by Schwarz and others [16, 17]. We will not describe the instrumentation at all, and readers are directed to the original articles for detailed experiment descriptions.

Ligand dissociation

Ligand dissociation is often the step that generates the active catalyst. Coordinatively saturated complexes tend to be unreactive until a vacant coordination site is produced by departure of a labile ligand, and this sort

of dissociation can be easily achieved in the gas phase by use of collision induced dissociation (CID). CID is the process that allows MS/MS (and MSn) experiments to be performed: an ion is isolated in the first stage of mass spectrometry, and accelerated within a cell filled with an inert gas (typically argon or some other noble gas). Energetic collisions with the gas deposit internal energy into the ion to the point that a bond breaks and unimolecular decomposition takes place, generating a neutral fragment and a charged product ion, and the latter can be detected in a second stage of mass spectrometry. Frequently, multiple ions are observed since more than one process can be accessible at a given energy (i.e., ion acceleration), and sequential fragmentations can also occur. Fortunately, most transition metal complexes decompose in a way that is predictable and often representative of their solution-phase chemistry, especially at the lowest energy levels. The first fragmentation event generates an ion that is usually due to dissociation of the most labile, L-type ligand in the complex. Loss of X-type ligands and especially multi-dentate ligands tends to be unusual (though in cases where it does occur, such observations are revealing of the chemistry of the complexes).

A simple example of sequential ligand dissociation is observed if CID is performed on metal carbonyl complexes. Carbon monoxide is easily liberated from such complexes, and by changing the collision energy, anywhere from none, to some, to all of the CO can be lost. Such experiments can be conveniently summarized by use of a three-dimensional plot of collision energy vs. *m/z*, with the intensity of the ion providing the height of the surface (Fig. 3) [18]. This type of presentation is known as "energy-dependent ESI-MS" (EDESI-MS) [19].

The more ligands removed from a complex, the more unsaturated and more reactive it becomes. For example, if all 13 CO ligands are removed from $[CoRu_3(CO)_{13}]^-$, it will even react with methane to produce a wide variety of hydrocarbon complexes [20].

The relative propensity of complexes to lose ligands can be probed *qualitatively* quite easily using CID. For example, rhodium complexes of the type $[Rh(PP)(\eta^6\text{-fluorobenzene})]^+$ (PP = chelating diphosphine

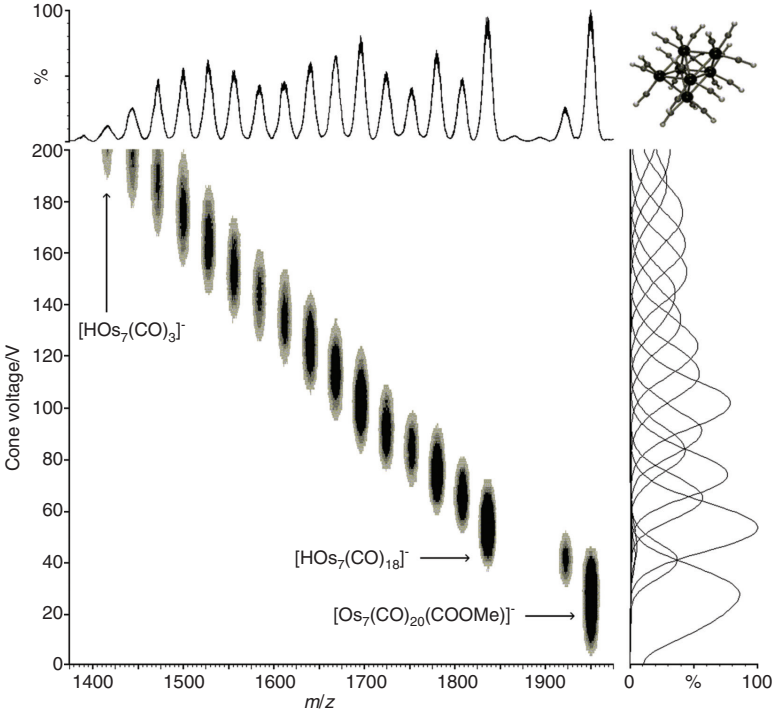

Fig. 3: Ligand loss from a heptanuclear osmium carbonyl cluster, derivatized by means of nucleophilic attack on a carbonyl ligand to generate a $[M + OMe]^-$ ion. The ion decomposes under CID conditions by an initial loss of CO, followed by rapid loss of H_2CO and then consecutive CO losses down to an $[HOs_7]^-$ core. Reprinted with permission from reference [18]. Copyright © 2002 John Wiley & Sons, Ltd.

ligand) possess an unusually weakly-bound fluorobenzene ligand, which is readily lost under CID conditions (Fig. 4) – a property reflected in its solution chemistry [21].

Quantitative comparisons are more involved, but are correspondingly more rewarding in that they allow bond strengths to be extracted from such studies. For example, Grubbs' first and second generation metathesis catalysts must dissociate a phosphine ligand to generate the active coordinatively-unsaturated 14 electron intermediate. As a result, the relative binding energy of the phosphine is a key bit of information in determining how kinetically important phosphine dissociation is to the turnover rate of the catalyst. Chen and coworkers used threshold collision-induced dissociation (TCID) experiments to measure the absolute activation energies of phosphine dissociation from charged-analogs of Grubbs first- and second-generation catalysts in the gas phase (Scheme 1) [22].

A triple quadrupole mass spectrometer modified with a custom 24-pole ion guide ensured pre-thermalization of the ions being studied: a requirement for the collection of accurate thermochemical data by mass spectrometry. The measured values (33.4 and 36.9 kcal/mol for the first generation system and second-generation system respectively) were particularly useful in validating claims about the accuracy of the M06-L functional for predicting dissociation energies in organometallic complexes.

Ligand association reactions

Simple ligand association reactions have not been the focus of many gas-phase studies. If ligand binding energies are the goal, they can be more easily and accurately determined by measuring the energy required for ligand dissociation [23]. Nevertheless, ligand association reactions are a very common feature of gas-phase experiments. They often precede the gas phase reaction of interest (for example the gas-phase oxidative addition of allyl acetate to copper likely occurs via initial allyl acetate coordination to copper through oxygen [24]), but most often they appear as "background reactions" in which residual water or solvent within

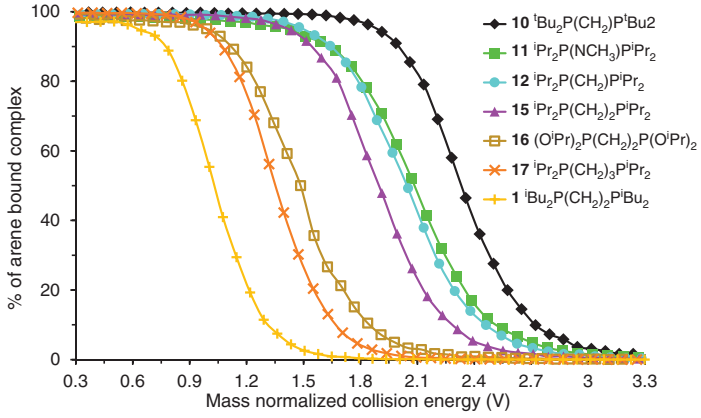

Fig. 4: CID data from MS/MS experiments on complexes of the type [Rh(PP)(η⁶-fluorobenzene)]⁺ (PP = chelating diphosphine ligand). Collision energy has been normalized to center of mass. Reprinted with permission from reference [21]. Copyright © 2014 Elsevier.

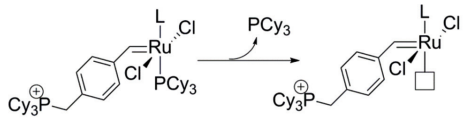

Scheme 1: Ligand dissociation from the first- or second-generation Grubbs catalyst.

the mass spectrometer coordinates to a coordinatively-unsaturated ion. These types of background reactions are most notable in ion trap instruments where the operating pressure is relatively high compared to other mass analyzers. For example, Fig. 5 shows a series of related metal complexes that react to varying degrees with background water in an ion trap [25].

Ligand exchange reactions

Removal of a ligand in the gas phase by CID generates a vacant coordination site, and if suitable replacement ligands are available, they can occupy the newly available spot. Such reactions can establish whether or not the rate of association of the incoming ligand is important, and CID of the product of the ligand association can establish whether or not further reaction has occurred. For example, the gas phase reactivity of $[Co_2(CO)_6(\mathbf{1})]^+$ (**1** = terminal alkyne with a pyrrolidinium group) with different alkenes was examined after dissociation of a single CO ligand, and all alkanes were found to react to a similar extent (see Fig. 6) [26]. Further CID resulted exclusively in alkene dissociation, providing evidence that further reactions such as insertion had not yet occurred (and thus suggesting a significant barrier exists for such processes).

Ligand scrambling phenomena can be important side-reactions in various catalytic processes. The Mizoroki-Heck reaction was recently investigated by ESI-MS/MS and gas-phase ion-molecule reactions [27]. The authors of this contribution orchestrated the Mizoroki-Heck reaction in the gas phase by ion-molecule reaction and CID and were able to measure the extent of the aryl/phenyl scrambling on the basis of the palladium-hydride complex ion abundances (Fig. 7), in an elegant and direct way of investigating this particular process.

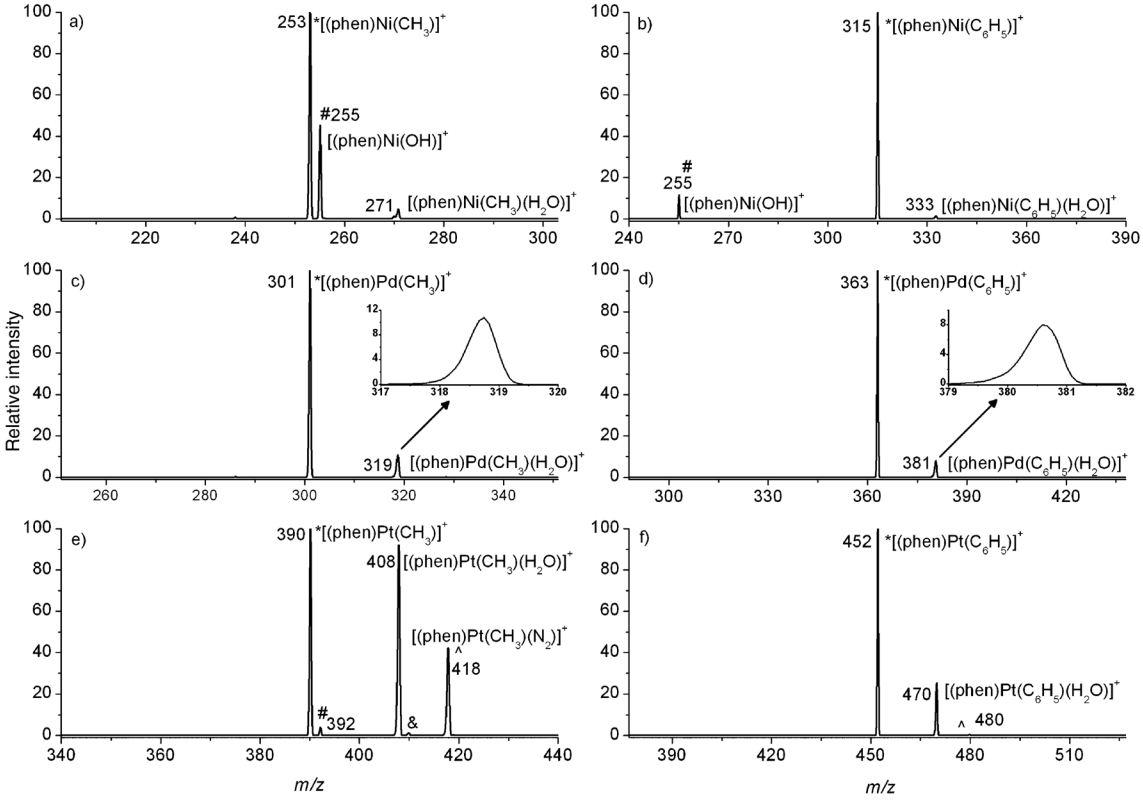

Fig. 5: Reactions of nickel, palladium and platinum organometallic complexes with background water in an ion trap mass spectrometer. Reprinted with permission from reference [25]. Copyright 2013 American Chemical Society.

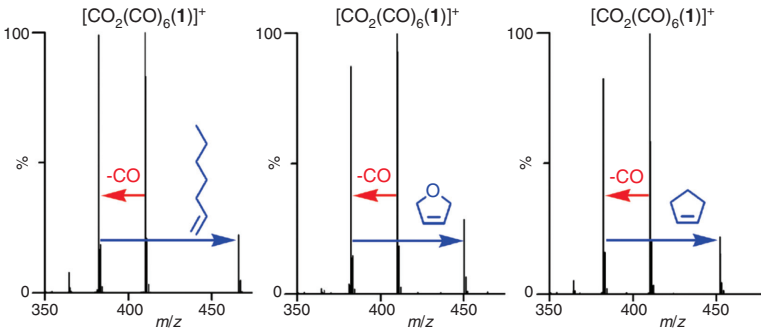

Fig. 6: Gas-phase reactions of $[Co_2(CO)_6(\mathbf{1})]^+$ with three different alkenes at a cone voltage of 20 V. In each case, one CO ligand is removed and the alkene adds to $[Co_2(CO)_5(\mathbf{1})]^+$. The alkene does not add to the fully saturated ion. Reprinted with permission from reference [26]. Copyright 2011 American Chemical Society.

Oxidative addition

One of the most popular examples, the oxidation of aryl halides to palladium(0) phosphine complexes is the proposed first step in a whole range of Pd-catalyzed cross coupling reactions, and although the process has been extensively studied in solution there are certain unavoidable limitations to the condensed-phase studies. Specifically, in a solution containing palladium phosphine complexes an equilibrium always exist between $Pd(PPh_3)_3$, $Pd(PPh_3)_2$ and even $Pd(PPh_3)$. So, which one is the true active catalyst? Gas-phase IMR studies within an ion trap allowed the isolation of each of these species individually (with the use of a charge-tagged phosphine) and their reactivity towards the aryl halides PhI, PhBr, PhCl and PhF was tested [28]. The results are shown in Fig. 8 for the mono- and bis-ligated palladium complexes and they clearly demonstrate that for all but PhI, the bis-ligated system is completely inactive towards oxidative addition and the mono-ligated complex is the more likely active species.

It is important to note that, since the observed reaction of PhX with the ionic palladium complex could correspond to true oxidative addition or just simple ion-molecule adduct formation, DFT calculations and additional MS experiments were crucial in arriving at the correct structural assignment. DFT indicated that the barriers for PhF and PhCl reactions were too high and that the observed species were adducts, and this was borne out in CID experiments that showed this $[Pd(PR_3)(PhX)]^-$ fragmented exclusively by loss of PhX.

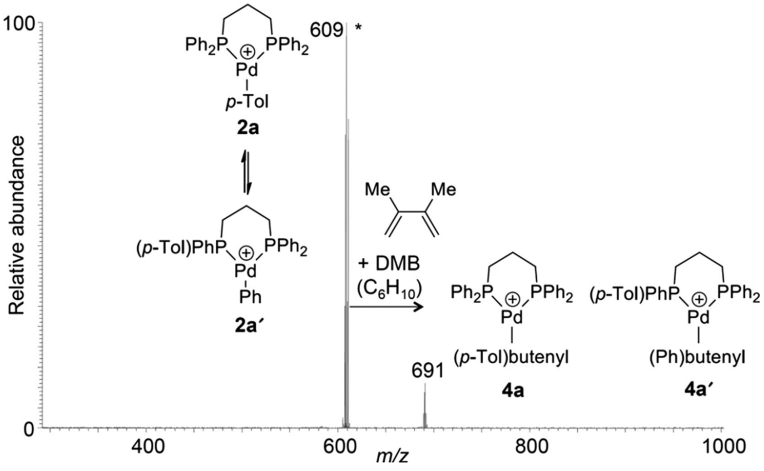

Fig. 7: Aryl migration during isolation of **2a** followed by ion-molecule reaction of **2a**/**2a′** with dimethylbutene to give a mixture of **4a** and **4a′**. The isobaric ions could be differentiated by CID as they β-eliminated different neutral products to generate different mass product ions. Reprinted with permission from reference [27]. Copyright © 2014 WILEY-VCH Verlag GmbH & Co. KGaA, Weinheim.

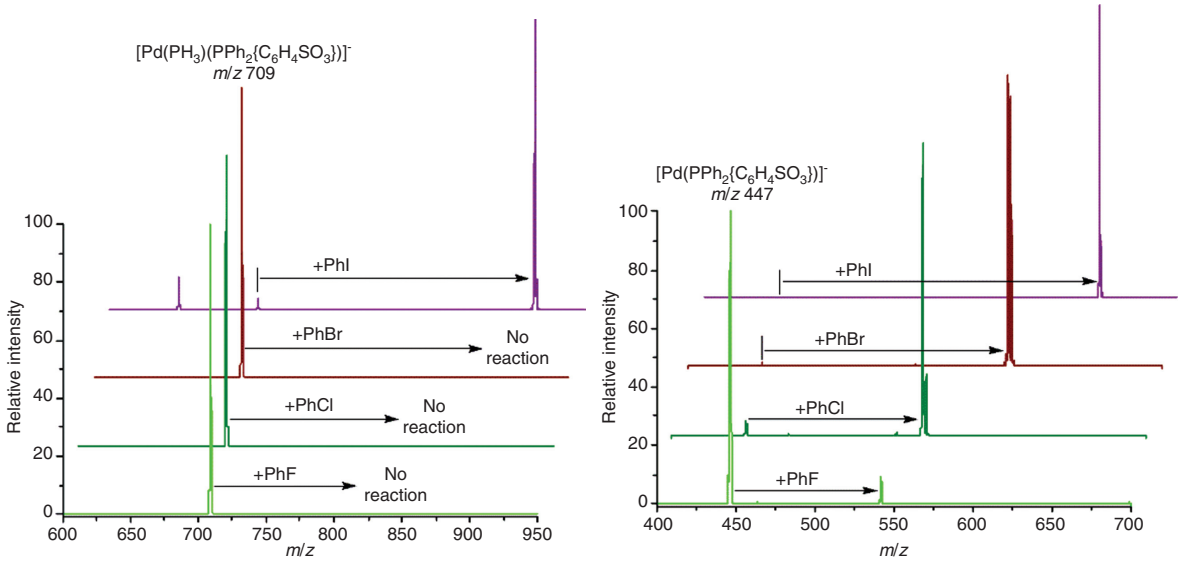

Fig. 8: Left: MS^2 mass spectra of the exposure of PhX, X = F, Cl, Br, and I to $[Pd(PPh_3)(PPh_2\{C_6H_4SO_3\})]^-$ (*m/z* 709) for a reaction time of 0.5 s. Right: MS^3 mass spectra of the exposure of PhX, X = F, Cl, Br, and I to $[Pd(PPh_2\{C_6H_4SO_3\})]^-$ (*m/z* 447) for 0.5 s. Reprinted with permission from reference [28]. Copyright © 2013 WILEY-VCH Verlag GmbH & Co. KGaA, Weinheim.

Conversely, the $[Pd(PR_3)(PhI)]^-$ complex fragmented exclusively by loss of PR_3, indictating that the precursor had in fact formed the $[Pd(PR_3)(Ph)(I)]^-$ oxidative addition product. PhBr produced a mixture of both products.

A similar oxidative addition reaction was studied by MS in order to solve an ongoing debate in the literature. In 2007 CeO_2-supported gold(I) was reported by Corma and coworkers as an alternative catalyst in the Sonogashira coupling reaction [29], but this claim was met with disbelief when a different group of researchers was unable to oxidatively add iodobenzene to a range of mononuclear Au(I) complexes [30]. They suggested that the initial results must have been due to palladium impurities. IMRs within a mass spectrometer can easily rule out such impurities by mass selecting the catalyst of interest. So, in 2012 O'Hair and coworkers studied the gas-phase reactivity of iodobenzene with the mononuclear gold(I) complex $[Au(PPh_3)_2]^+$ and ligated gold clusters $[Au_3L^n]^+$ where $L^n = Ph_2P(CH_2)_nPPh_2$ (Scheme 2) [31].

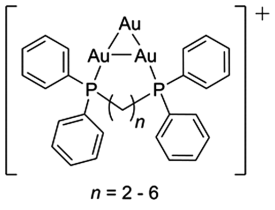

Scheme 2: Ligated cationic gold clusters studied in the gas phase.

Table 1: Kinetics of the IMRs of ligated gold cations with iodobenzene.

Reactant	Product (BR)	k_{expt} [a]	Reaction efficiency
$(PPh_3)_2Au^+$	N.R.		
$[Au_3L^3]^+$	$[Au_3L^3(Ph)(I)]$+ (100 %)	3.57×10^{-13}	0.04
$[Au_3L^4]^+$	$[Au_3L^4(Ph)(I)]$+ (100 %)	6.55×10^{-12}	0.75
$[Au_3L^5]^+$	$[Au_3L^5(Ph)(I)]$+ (100 %)	8.66×10^{-11}	9.9
$[Au_3L^6]^+$	$[Au_3L^6(Ph)(I)]$+ (100 %)	3.69×10^{-10}	42

BR, branching ratio; N.R., no reaction. L^n indicates the bidentate phosphine ligand depicted in Scheme 2 where n = 2–6.
[a]In units $cm^3\ mol^{-1}\ s^{-1}$.

Kinetic analysis of the gas-phase reactions with iodobenzene (Table 1) showed that while the bis-ligated mononuclear gold(I) was inactive with respect to oxidative addition, the ligated gold clusters were active. This was consistent with new kinetic studies carried out by Corma which implicated gold clusters as the active catalyst.

In addition, the linker size of the bisphosphine ligand was found to have a significant effect on the reactivity of the gold cluster. With the help of DFT calculations O'Hair and coworkers were able to identify the key structural differences in the transition states for oxidative addition that influenced the rate of the reaction.

β-hydride elimination

β-hydride elimination is the reverse of an insertion of an unsaturated substrate into a metal hydride bond. It is responsible for alkyl complexes with hydrogens on the beta carbon being unstable, and consistently stable alkyl complexes only became well-known after this transformation was understood. Gas-phase reactions involving these decompositions therefore have most commonly involved generating the complexes in the gas phase by some other process, then observing the elimination of the unsaturated moiety. For example, in unpublished work, we found that the alkyl iodides MeI, EtI and BuI all reacted readily with $[Pd(PPh_2\{C_6H_4SO_3\})]^-$ (see section above on oxidative addition), but only the methyl iodide generated an alkyl complex $[Pd(PPh_2\{C_6H_4SO_3\})(R)(I)]^-$; the other two produced only the hydride complexes $[Pd(PPh_2\{C_6H_4SO_3\})(H)(I)]^-$; revealing that alkene elimination had occurred. There are many published examples of β-hydride elimination from the O'Hair laboratory, who often generate alkyl complexes through decarboxylation of carboxylate ligands [32–34]. These new alkyl complexes containing beta-hydrogens, unstable in solution, are prone to alkene elimination in the gas phase. The Mizoroki–Heck example alluded to in the ligand exchange reaction also exemplifies the β-hydride elimination to generate the final product [27].

Migration (insertion)

Insertion reactions are a fundamental part of organometallic chemistry, and while formally described as insertions, these generally proceed by migration of one ligand on to another (e.g., the formal reverse of a beta-hydride elimination). In order for such reactions to be directly studied by ESI-MS, a mass change must be involved, so the migration event can be trapped by the gas-phase reagent. Indirect evidence of insertion has been established in cases such as in the insertion of a benzyne ligand into an N–H bond on an adjacent ligand [35]. The product of this reaction was made independently and the two species were shown to have identical MS^3 spectra.

Schäfer's demonstration of a gas-phase Heck reaction [36] is an example of sequential insertion and β-elimination steps. Initially, a tri(2-furyl)phosphine ligand was substituted for isoprene in the gas phase, and subsequent elimination of a fragment of *m/z* 202 pointed to migration of the aryl ligand onto the isoprene ligand and beta-elimination of the coupled product (Fig. 9).

Multiple insertions can be observed in cases where the metal complex is highly reactive, such as olefin polymerization catalysts. Santos and Metzger [37] showed that cationic zirconocene complexes of the type $[Cp_2ZrR]^+$ (R = alkyl) readily insert ethylene multiple times in the gas phase to generate $[Cp_2Zr(CH_2CH_2)_nR]^+$ complexes (Fig. 10), in an exact duplicate of the chemistry such complexes exhibit in solution to generate polyethylene.

Addition reactions

Organometallic complexes can be susceptible to both nucleophilic and electrophilic addition reactions, and such reactions can be useful for the purposes of characterizing compounds by ESI-MS. For example, neutral

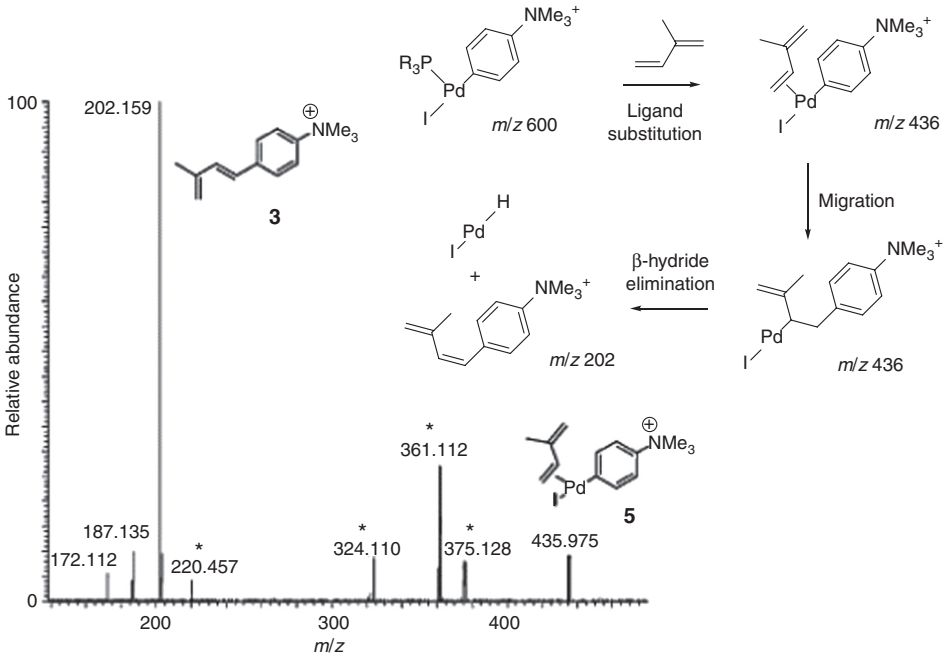

Fig. 9: LTQ-MS^3 product ion spectrum of isoprene adduct ion of *m/z* 436. Reprinted with permission from reference [36]. Copyright © 2011 Elsevier.

metal carbonyl complexes are usually invisible to ESI-MS, but addition of small quantities of sodium methoxide generates $[M+OMe]^-$ ions, via nucleophilic attack of $[OMe]^-$ on the electropositive carbon atom of one of the carbonyl ligands [38, 39]. However, study of such reactions in the gas phase would likely necessitate the metal complex to be charged and the nucleophile to be neutral, based on volatility arguments. Reaction with a charged nucleophile could perhaps be achieved with organometallic molecules such as $Ni(CO)_4$ or $Fe(CO)_5$ (both low boiling point liquids), but has not to our knowledge been performed. Cationic metal complexes

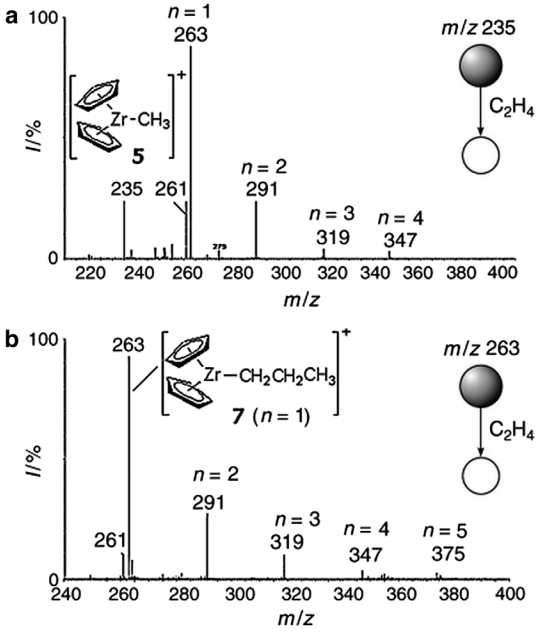

Fig. 10: Gas-phase reactivity of $[Cp_2Zr(CH_3)]^+$ with ethylene, exhibiting multiple insertions of ethylene into a metal-carbon bond. Reprinted with permission from reference [37]. Copyright © 2006 WILEY-VCH Verlag GmbH & Co. KGaA, Weinheim.

react very readily with charged nucleophiles, but the number of examples with neutral nucleophiles is much fewer [40].

Gas phase electrophilic additions suffer from the same restrictions as their nucleophilic brethren. Electrophiles of the type RI have been shown to react with $[CH_3CuR]^-$ complexes, but via an oxidative addition/reductive elimination pathway [41].

Gas phase cycloaddition reactions have been studied with success. Schäfer and co-workers reacted a mixture of gaseous phenylacetylene and isoprene with the isolated ion $[Co(dppe)]^+$ (dppe = 1,2-bis(diphenylphosphino)ethane) in the gas phase to generate [Co(dppe)(isoprene)(phenylacetylene)]$^+$. CID of this ion resulted in the Diels–Alder reaction occurring to generate [Co(I)(dppe)(1-methyl-4-phenylcyclohexadiene)]$^+$, whose existence was established by the release of the neutral $C_{13}H_{14}$ product from the precursor ion [42].

Transmetallation

Transmetallation is the process by which a (usually) alkyl or aryl ligand is swapped from one metal to another, and is particularly well-known in cross-coupling reactions. It is a challenge to conduct this elementary step in the gas phase because at least one reagent must be volatile, and that is not often easy to achieve. However, the Chen group circumvented this by starting from solution with two metal centers already forming an adduct [43]. Transmetallation of methyl groups from platinum(II) to gold(I) was directly observed for the first time by studying the unimolecular gas-phase reactions of the heterobimetallic complexes $\{[(dmpe)PtMe_2]AuPR_3\}^+$ where dpme = 1,2-bis(dimethylphosphino)ethane and R = methyl, phenyl or tertiary-butyl. Threshold CID experiments on the heterobimetallic complex led to two fragmentation pathways consistent with (1) simple methyl transfer to gold resulting in $[(dmpe)PtMe]^+$ and $MeAuPR_3$ or (2) methyl transfer with concerted back-transfer of the monodentate phosphine ligand to give $[(dmpe)Pt(Me)(PR_3)]^+$ and AuMe (Scheme 3).

The details of these pathways were confirmed by extensive DFT calculations and the L-CID program was used to fit the experimental TCID data in order to extract energy barriers of 22.3 ± 0.9 kcal mol^{-1} for reaction channel (1), and 47.9 ± 1.8 kcal mol^{-1} for reaction channel (2) when R = Ph. Moreover, ^{31}P NMR-monitoring of the reaction between R_3PAuCl and $[(dmpe)Pt(Me)_2]$ in solutions of THF-d_8 with $Na[BAr^F_4]$ as a halide abstracting agent revealed that the analogous pathways operate in solution.

Metathesis

An early example of a gas-phase MS experiment that is directly relevant to solution-phase reactivity came from the Chen group in 1998 [44]. They examined the solution-phase olefin metathesis catalyst $[RuCl_2(=CHR)(PCy_2R')]^+$ where R′ is a charge-tag on the phosphine ligand that allows visualization of the otherwise neutral complex. The catalyst was electrosprayed into a 24-pole reaction chamber filled with a low pressure of norbornene and any resulting products were characterized by a subsequent quadrupole mass analyser. When R = CH_2CH_3, up to three additions of norbornene were observed to occur in the time it took the catalyst to travel from one end of the reaction chamber to the other (Scheme 4).

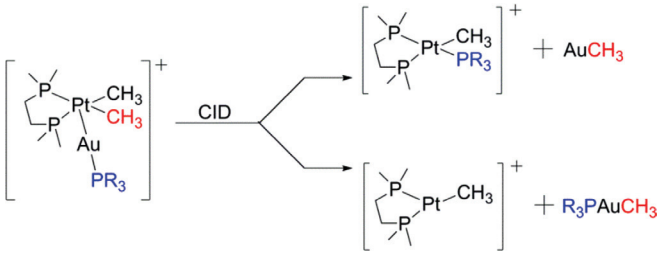

Scheme 3: Reaction scheme for CID of $\{[(dmpe)PtMe_2]AuPR_3\}^+$ (*m/z* 834).

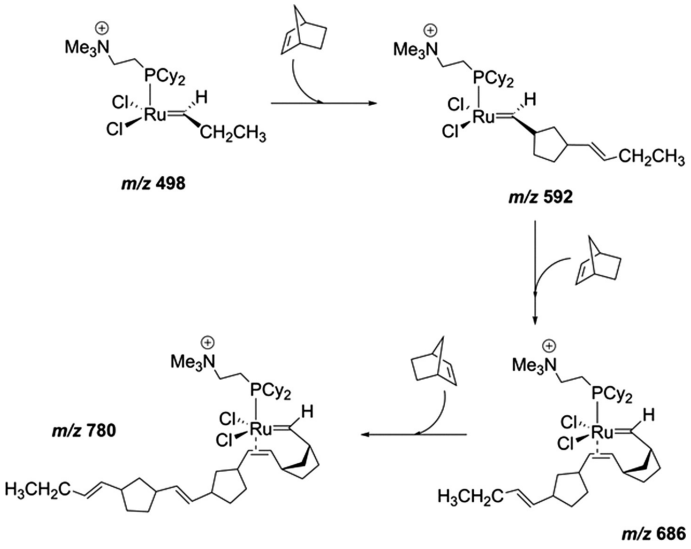

Scheme 4: Ring-opening metathesis of norbornene in a mass spectrometer.

Relative rate constants were measured for this system and a number of others and although the absolute rates were much faster in the gas-phase, the general reactivity trends tracked well with the analogous solution-phase reactions.

Oxidation

Oxygen is reactive towards many organometallic compounds, and there are many catalytic reactions using oxygen as a reagent. An example of a gas-phase reaction between an anionic metal carbonyl cluster and O_2 is shown in Fig. 11, though in fairness, this is perhaps better described as a gas-phase incineration rather than

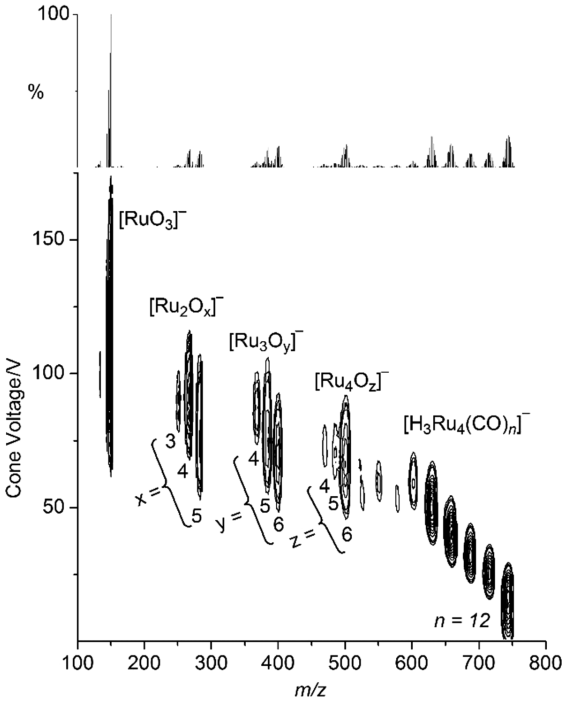

Fig. 11: EDESI-MS of the reaction of $[H_3Ru_4(CO)_n]^-$ (n = 0–12) with O_2(g). Adapted from reference [45].

a reaction: at a certain point, combination of O_2 and the unsaturated cluster results in complete stripping of all CO ligands and a rendering of the cluster down to mono- and polynuclear ruthenium oxides of the form $[Ru_xO_y]^-$ (x = 1–4, y = 3–6) [45]. No evidence of combinations of CO and O as ligands was obtained, so reactions following O_2 addition are clearly rapid. Ultimately, the fragment $[RuO_3]^-$ dominates, corresponding to Ru in the +5 oxidation state.

Clustering

Formation of clusters is usually a side-reaction in catalytic reactions, but understanding how any decomposition pathway occurs is important when designing good catalysts. Studying such reactions in the gas phase is hindered by the fact that at such low pressures clustering is statistically improbably. However, the microscopic reverse of clustering events can be examined if clusters from solution can be gently transferred into the gas phase without fragmentation. For example, experiments have been conducted with anionic metal carbonyl clusters and $Fe(CO)_5$ in the gas phase where a variety of higher nuclearity species were successfully isolated from solution (Fig. 12) [46].

Deinsertion/elimination

There are a number of common methods for forming new metal carbon bonds via deinsertion reactions at a metal center – namely, decarboxylation of a metal carboxylate (Scheme 5A), desulfination of a metal sulfinate (Scheme 5B) or desulfonation of a metal sulfonate (Scheme 5C) – and these processes are often used in metal catalyzed C–C bond forming reactions to generate an activated coupling partner.

O'Hair and coworkers have used gas-phase reactions to compare the intrinsic ability of the three processes named above to generate organocuprates [47]. Under CID conditions the three ligands were pitted directly against each other. For example, the complex $[Me\mathbf{CO_2}Cu\mathbf{O_2S}Me]^-$ exclusively eliminates SO_2, while the complex $[Me\mathbf{CO_2}Cu\mathbf{O_3S}Me]^-$ strongly favours loss of CO_2. For copper systems it was concluded that desulfination occurs more easily than decarboxylation, which in turn, is more facile than desulfination.

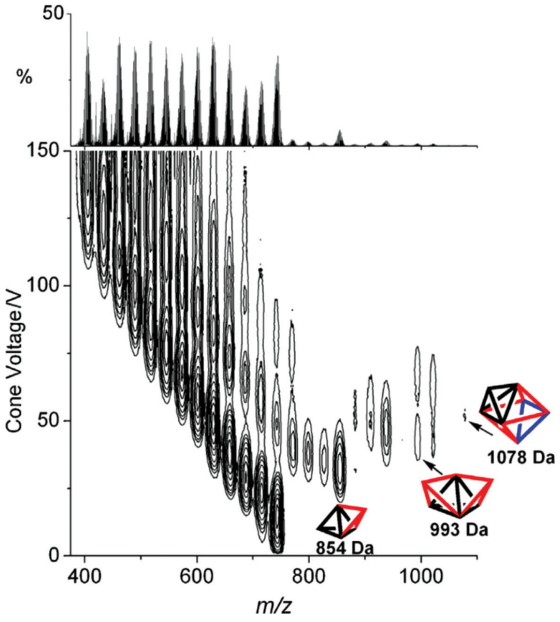

Fig. 12: EDESI-MS of the reaction of $[H_3Ru_4(CO)_n]^-$ (n = 0–12) with $Fe(CO)_5$(g). Reprinted with permission from reference [46]. Copyright © 2013 Elsevier.

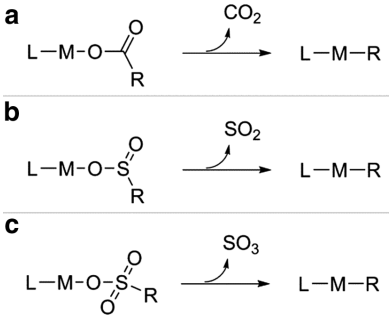

Scheme 5: Common deinsertion reactions for generating new metal carbon bonds.

Quantitative gas-phase unimolecular reactions have been used to predict the cyclopropanation ability of various gold-carbene precursor complexes based on their ability to eliminate a leaving group and form the active metal-carbene [48]. The bond dissociation energies (BDEs) for gold-carbene formation from complexes A, B and C were measured by threshold CID experiments (Scheme 6).

The trend in S–C bond strength (A < C < B) accurately predicted how well the complex would cyclopropanate para-methoxystyrene in solution (A > C > B). However the correlation was not linear. Small changes in BDEs led to huge changes in product yield (<5 %–99 %): likely because for the less reactive precursors other decomposition pathways became competitive in solution. Nevertheless, the information gained in these experiments provides clear insights into how various structural perturbations affect the reactivity of these of gold complexes both in the gas- and solution- phase and enabled the rational design of better gold carbene precursors.

Reductive elimination

Reductive eliminations (RE) can be challenging to study conventionally, for the simple reason that complexes set up to undergo RE tend to be unstable with respect to exactly that process. However, ESI-MS is sufficiently sensitive that even very low concentrations of fleeting intermediates can be isolated and examined by CID. Because RE is a unimolecular decomposition, no reagent gas is required, just the collision gas to raise the internal energy of the ion to the point where RE is induced. The facility of the process is revealed first by whether it happens at all: for complexes with other ligands, other fragmentation pathways (notably ligand dissociation) may occur preferentially to RE. For example, oxidative addition of aryl iodides to Pd(0) bisphosphine complexes generated (L)Pd(II)(Ar)(I) complexes, which are not prone to reductive elimination but instead simply dissociate a phosphine ligand under CID conditions. On the other hand, the same complexes but with I swapped for a $-C_2Ph$ ligand do readily reductively eliminate ArC_2Ph, and the extent to which they do so is affected by the electronic properties of the aryl ligand (Fig. 13) [49].

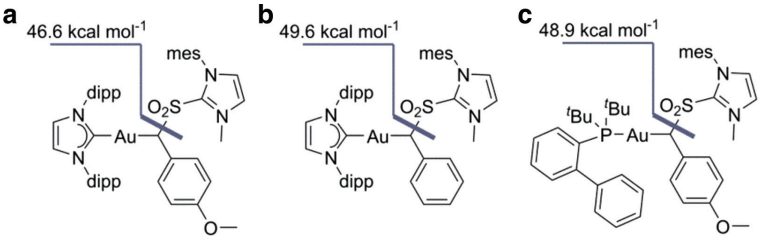

Scheme 6: The energy required to form gold carbenes by TCID from their precursors a, b and c in the gas phase is predictive of the cyclopropanation ability of the complexes in solution. mes, 1,3,5-trimethylphenyl; DIPP, diisopropylphenyl; tBu, tertiary butyl.

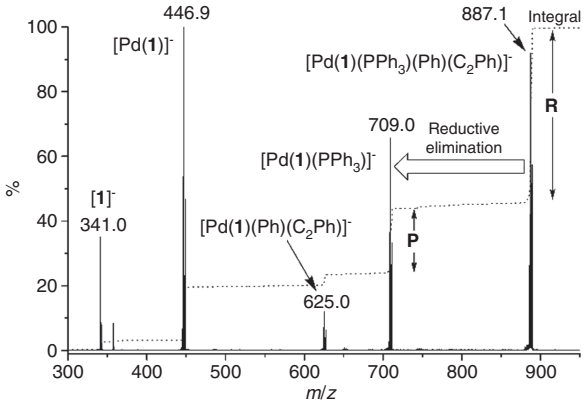

Fig. 13: Negative-ion ESI-MS/MS of $[Pd(PPh_2\{m\text{-}C_6H_4SO_3\})(PPh_3)(Ph)(C_2Ph)]^-$, showing reductive elimination of PhC_2Ph, at a collision voltage of 15 V. Reproduced by permission of The Royal Society of Chemistry from reference [49].

An elegant study on tetraalkylcuprates allowed an up-close examination of reductive elimination from various species related to classic Gillman reagents and highlights the ability of gas phase studies to reveal the effect of counterions at a molecular level [50]. Koszinowski and coworkers used ESI-MS to examine complexes of the form $[CuMe_3R]^-$ and $[Cu_2Me_6RR'Li]^-$ (Scheme 7) which were extracted directly from solution-phase mixtures of MeLi, CuCN, and the appropriate organyl halide.

Due to the moisture sensitivity of these complexes care was taken to dry the ESI source region using dry solvents and high nebulizing and drying N_2 gas flows. CID experiments resulted in reductive elimination from these centers and both homo- and hetero-coupling products were observed. Interestingly, the presence of a Li^+ counterion in the complexes $[Cu_2Me_6RR'Li]^-$ strongly favors heterocoupling. Supporting theoretical

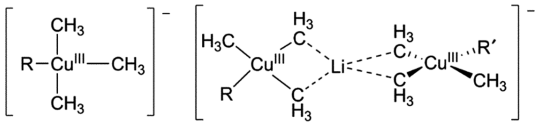

R/R′= Et, Pr, Bu, CH_2CH_2Ph, $CH_2CH{=}CH_2$

Scheme 7: Examples of catalytically relevant Cu(III) complexes observed by ESI-MS.

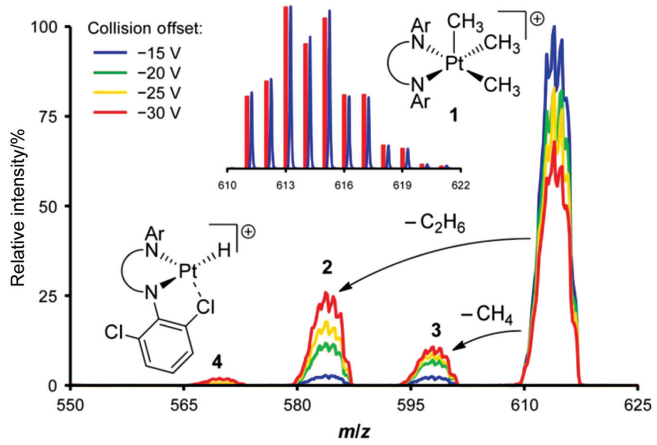

Fig. 14: TCID of $[(NN)Pt^{IV}Me_3]^+$ (NN = α-diimine). Note that the MS signals shown here are much broader than those for standard MS spectra. This is to ensure that the energy of the ions is not unintentionally raised by the isolation process. Reprinted with permission from reference [51]. Copyright 2014 American Chemical Society.

calculations suggest a possible explanation: the lithium cation preferentially interacts with the methyl groups of the copper complexes thus preventing them from participating in reductive elimination.

Reductive elimination, being a unimolecular process, lends itself particulary well to quantitative TCID measurements. This elementary reaction is also relatively non-polar which suggests that quantitative gas-phase measurements of the reductive elimination process will give a reasonable indication of the analogous solution-phase chemistry. Recently the Chen group has measured the reductive elimination of alkanes from Pt(IV) (Fig. 14) and the threshold energy for the reductive elimination of ethane was calculated to be 22.9 kcal mol^{-1} [51]. Although there has been no directly comparable solution-phase study, the gas-phase findings are consistent with what is known of similar solution-phase systems.

A similar semi-quantitative study has been conducted for palladium(IV) complexes [52].

Conclusions

Gas-phase reactions offer a unique opportunity to isolate the elementary steps that make up a catalytic cycle, and study these steps free from the influence of solvent. Nearly all such steps that are typically found in organometallic reactions have been studied in this way, and many have provided unique insights. Any modern instrument with MS/MS capability can study unimolecular reactions, and while the capability to perform the bimolecular reactions is not yet present on commercial instruments, the modifications required to achieve them are minor. The fact that gas-phase reactions are so neatly complementary to computational approaches to understanding reactivity, and the fact that they can be used to help fill in the gaps in a catalytic cycle that cannot be revealed from real-time monitoring methods, together combine to make the future for this approach highly promising.

Acknowledgments: JSM thanks NSERC (Discovery and Discovery Accelerator Supplement) for operating funds, and CFI, BCKDF and the University of Victoria for infrastructural support. KLV thanks NSERC and the ETH for Postdoctoral Fellowships.

References

[1] L. P. E. Yunker, R. L. Stoddard, J. S. McIndoe. *J. Mass Spectrom.* **49**, 1 (2014).
[2] P. J. Dyson, J. S. McIndoe. *Inorg. Chim. Acta.* **354**, 68 (2003).
[3] A. T. Lubben, J. S. McIndoe, A. S. Weller. *Organometallics* **27**, 3303 (2008).
[4] D. M. Chisholm, A. G. Oliver, J. S. McIndoe. *Dalton Trans.* **2010**, 364 (2010).
[5] M. A. Henderson, J. S. McIndoe. *Chem. Commun.* **2006**, 2872 (2006).
[6] D. M. Chisholm, J. S. McIndoe. *Dalton Trans.* **2008**, 3933 (2008).
[7] J. Limberger, B. C. Leal, A. L. Monteiroa, J. Dupont. *Chem. Sci.* **6**, 77 (2015).
[8] K. L. Vikse, Z. Ahmadi, J. Luo, N. van der Wal, K. Daze, N. Taylor, J. S. McIndoe. *Int. J. Mass Spectrom.* **323–324**, 8 (2012).
[9] D. Agrawal, D. Schroder. *Organometallics* **30**, 32 (2011).
[10] L. S. Santos. *J. Braz. Chem. Soc.* **22**, 1827 (2011).
[11] K. L. Vikse, Z. Ahmadi, J. S. McIndoe. *Coord. Chem. Rev.* **279**, 96 (2014).
[12] C. H. Beierlein, B. Breit, R. A. Paz-Schmidt, D. A. Plattner. *Organometallics* **29**, 2521 (2010).
[13] M. A. Schade, J. E. Fleckenstein, P. Knochel, K. Koszinowski. *J. Org. Chem.* **75**, 6848 (2010).
[14] K. L. Vikse, M. P. Woods, J. S. McIndoe. *Organometallics* **29**, 6615 (2010).
[15] Z. Ahmadi, J. S. McIndoe. *Chem. Commun.* **49**, 11488 (2013).
[16] K. Eller, H. Schwarz. *Chem. Rev.* **91**, 1121 (1991).
[17] L. Operti, R. Rabezzana. *Mass Spectrom. Rev.* **25**, 483 (2006).
[18] C. P. G. Butcher, P. J. Dyson, B. F. G. Johnson, J. S. McIndoe, P. R. R. Langridge-Smith, C. Whyte. *Rapid Commun. Mass Spectrom.* **16**, 1595 (2002).
[19] P. J. Dyson, B. F. G. Johnson, J. S. McIndoe, P. R. R. Langridge-Smith, *Rapid Commun. Mass Spectrom.* **14**, 311 (2000).
[20] C. P. G. Butcher, A. Dinca, P. J. Dyson, B. F. G. Johnson, P. R. R. Langridge-Smith, J. S. McIndoe. *Angew. Chem. Int. Ed.* **42**, 5752 (2003).

[21] S. D. Pike, I. Pernik, R. Theron, J. S. McIndoe, A. S. Weller. *J. Organomet. Chem.* (2014). DOI: 10.1016/j.jorganchem.2014.08.012.
[22] S. Torker, D. Merki, P. Chen. *J. Am. Chem. Soc.* **130**, 4808 (2008).
[23] S. Naranicic, A. Bach, P. Chen. *J. Phys. Chem.* **111**, 7006 (2007).
[24] H. A. Sharif, K. L. Vikse, G. N. Khairallah, R. A. J. O'Hair. *Organometallics* **32**, 5416 (2013).
[25] M. J. Wooley, G. N. Khairallah, G. da Silva, P. S. Donnelly, B. F. Yates, R. A. J. O'Hair. *Organometallics* **32**, 6931 (2013).
[26] M. A. Henderson, J. Luo, A. Oliver, J. S. McIndoe. *Organometallics* **30**, 5471 (2011).
[27] L. Fiebig, N. Schlörer, H.-G. Schmalz, M. Schäfer. *Chem. Eur. J.* **20**, 4906 (2014).
[28] K. Vikse, T. Naka, J. S. McIndoe, M. Besora, F. Maseras. *ChemCatChem.* **5**, 3604 (2013).
[29] C. González-Arellano, A. Abad, A. Corma, H. García, M. Iglesias, F. Sánchez. *Angew. Chem. Int. Ed.* **46**, 1536 (2007).
[30] T. Lauterbach, M. Livendahl, A. Rosellon, P. Espinet, A. M. Echavarren. *Org. Lett.* **12**, 3006 (2010).
[31] P. S. D. Robinson, G. N. Khairallah, G. da Sliva, H. Lioe, R. A. J. O'Hair. *Angew. Chem. Int. Ed.* **51**, 3812 (2012).
[32] N. Rijs, T. Waters, G. N. Khairallah, R. A. J. O'Hair. *J. Am. Chem. Soc.* **130**, 1069 (2008).
[33] N. J. Rijs, R. A. J. O'Hair. *Organometallics* **28**, 2684 (2009).
[34] K. Vikse, G. N. Khairallah, J. S. McIndoe, R. A. J. O'Hair. *Dalton Trans.* **42**, 6440 (2013).
[35] Y. Chai, S. Shen, G. Weng, Y. Pan. *Chem. Commun.* **50**, 11668 (2014).
[36] L. Fiebig, H. Schmalz, M. Schäfer. *Int. J. Mass Spectrom.* **308**, 307 (2011).
[37] L. S. Santos, J. O. Metzger. *Angew. Chem. Int. Ed.* **45**, 977 (2006).
[38] W. Henderson, J. S. McIndoe, B. K. Nicholson, P. J. Dyson. *Chem. Commun.* **1996**, 1183 (1996).
[39] W. Henderson, J. S. McIndoe, B. K. Nicholson, P. J. Dyson. *J. Chem. Soc. Dalton Trans.* **1998**, 519 (1998).
[40] S. G. Davies, M. L. H. Green, D. M. P. Mingos. *Tetrahedron.* **34**, 3047 (1978).
[41] N. J. Rijs, N. Yoshikai, E. Nakamura, R. A. J. O'Hair. *J. Org. Chem.* **79**, 1320 (2014).
[42] L. Fiebig, J. Kuttner, G. Hilt, M. C. Schwarzer, G. Frenking, H.-G. Schmalz, M. Schäfer. *J. Org. Chem.* **78**, 10485 (2013).
[43] D. Serra, M.-E. Moret, P. Chen. *J. Am. Chem. Soc.* **133**, 8914 (2011).
[44] C. Hinderling, C. Aldhart, P. Chen. *Angew. Chem. Int. Ed.* **37**, 2685 (1998).
[45] M. A. Henderson, S. Kwok, J. S. McIndoe. *J. Am. Soc. Mass Spectrom.* **20**, 658 (2009).
[46] M. A. Henderson, J. S. McIndoe. *Int. J. Mass Spectrom.* **354–355**, 257 (2013).
[47] L. O'Connor Sraj, G. N. Khairallah, G. da Silva, R. A. J. O'Hair. *Organometallics* **31**, 1801 (2012).
[48] D. H. Ringger, I. J. Kobylianskii, D. Serra, P. Chen. *Chem. Eur. J.* **20**, 14270 (2014).
[49] K. L. Vikse, M. A. Henderson, A. G. Oliver, J. S. McIndoe. *Chem. Commun.* **46**, 7412 (2010).
[50] A. Putau, H. Brand, K. Koszinowski. *J. Am. Chem. Soc.* **134**, 613 (2012).
[51] E. P. A. Couzijn, I. J. Kobylianskii, M.-E. Moret, P. Chen. *Organometallics* **33**, 2889 (2014).
[52] J. Hývl, J. Roithová. *Org. Lett.* **16**, 200 (2014).